Estimation of volume flow in curved tubes based on analytical and computational analysis of axial velocity profiles

Estimation of volume flow in curved tubes based on analytical and computational analysis of axial velocity profiles

A. C. Verkaik, B. W. A. M. M. Beulen, A. C. B. Bogaerds,
M. C. M. Rutten, and F. N. van de Vosse
Department of Biomedical Engineering, Eindhoven University of Technology, P.O. Box 513, 5600 MB Eindhoven, The Netherlands

(Received 5 June 2008; accepted 29 December 2008; published online 13 February 2009)

To monitor biomechanical parameters related to cardiovascular disease, it is necessary to perform correct volume flow estimations of blood flow in arteries based on local blood velocity measurements. In clinical practice, estimates of flow are currently made using a straight-tube assumption, which may lead to inaccuracies since most arteries are curved. Therefore, this study will focus on the effect of curvature on the axial velocity profile for flow in a curved tube in order to find a new volume flow estimation method. The study is restricted to steady flow, enabling the use of analytical methods. First, analytical approximation methods for steady flow in curved tubes at low Dean numbers (Dn) and low curvature ratios (δ) are investigated. From the results a novel volume flow estimation method, the cos θ-method, is derived. Simulations for curved tube flow in the physiological range ($1 \leq \mathrm{Dn} \leq 1000$ and $0.01 \leq \delta \leq 0.16$) are performed with a computational fluid dynamics (CFD) model. The asymmetric axial velocity profiles of the analytical approximation methods are compared with the velocity profiles of the CFD model. Next, the cos θ-method is validated and compared with the currently used Poiseuille method by using the CFD results as input. Comparison of the axial velocity profiles of the CFD model with the approximations derived by Topakoglu [J. Math. Mech. **16**, 1321 (1967)] and Siggers and Waters [Phys. Fluids **17**, 077102 (2005)] shows that the derived velocity profiles agree very well for $\mathrm{Dn} \leq 50$ and are fair for $50 < \mathrm{Dn} \leq 100$, and this result applies for $0.01 \leq \delta \leq 0.16$, while Dean's [Philos. Mag. **5**, 673 (1928)] approximation only coincides for $\delta = 0.01$. For higher Dean numbers ($\mathrm{Dn} > 100$), no analytical approximation method exists. In the position of the maximum axial velocity, a shift toward the inside of the curve is observed for low Dean numbers, while for high Dean numbers, the position of the maximum velocity is located at the outer curve. When the position of the maximum velocity of the axial velocity profile is given as a function of the Reynolds number, a "zero-shift point" is found at $\mathrm{Re} = 21.3$. At this point the shift in the maximum axial velocity to the outside of the curve, caused by the difference in axial pressure gradient, balances the shift to the inside of the curve, caused by the centrifugal forces (radial pressure gradient). Comparison of the volume flow estimation of the cos θ-method with the Poiseuille method shows that for $\mathrm{Dn} \leq 100$ the Poiseuille method is sufficient, but for $\mathrm{Dn} \geq 100$ the cos θ-method estimates the volume flow nearly three times better. For $\delta = 0.01$ the maximum deviation from the exact flow is 4% for the cos θ-method, while this is 12.7% for the Poiseuille method in the plane of symmetry. The axial velocity profile measured at a certain angle from the symmetry plane results in a maximum estimation error of 6.2% for $\mathrm{Dn} = 1000$ and $\delta = 0.16$. The results indicate that the estimation of the volume flow through a curved tube from a given asymmetrical axial velocity profile is more precise with the cos θ-method than the Poiseuille method, which is currently used in clinical practice. © *2009 American Institute of Physics*. [DOI: 10.1063/1.3072796]

I. INTRODUCTION

A. Motivation and aim

Cardiovascular disease (CVD) is the number one cause of death in western society; it is responsible for nearly half (49%) of all deaths in Europe.[1] The main characteristic changes in arteries related to CVD are stiffening of the arteries, leading to an elevated blood pressure, and the thickening of the artery walls.[2] To obtain local hemodynamic variables and to deduce the important biomechanical parameters that are related to the development of CVD, such as compliance, wall shear stress, pulse wave velocity, and vascular impedance, the pressure and flow at specific areas of the blood circulation need to be monitored, preferably simultaneously and noninvasively.

For more than 50 years, ultrasound measurements have been used clinically to investigate patients noninvasively. From the measurements, various geometric and hemodynamic variables, such as velocity profiles, vessel diameter, intima-media thickness, wall shear stress, and pulse wave velocity, can be obtained.[3] Frequently used methods to determine blood flow velocity in the arteries by means of ultrasound are based on Doppler or cross correlation to assess axial velocity profiles.[4] Although the velocity profiles are

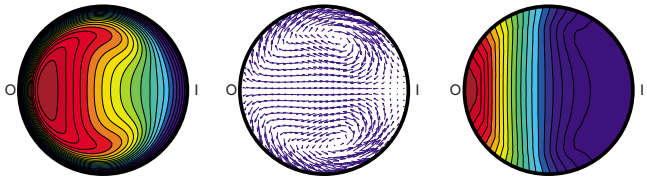

FIG. 1. (Color online) An example of the axial velocity distribution in a curved tube (left), the corresponding secondary velocity profile (middle), and the pressure distribution (right) obtained from CFD simulations, where "O" marks the outside of the curve and "I" the inside of the curve.

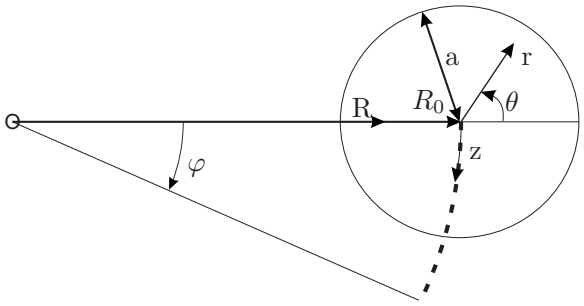

FIG. 2. The toroidal coordinate system (r,θ,z) with velocities (u,v,w), which is used to describe flow in a curved tube. The z-coordinate is defined as $z=R_0\varphi$, where R_0 is the curvature radius of the tube, a is the radius of the tube, and R is the distance to the center of curvature, defined as $R_0-a<R<R_0+a$. In this system u is the velocity in the r-direction, v is the velocity in the θ-direction and perpendicular to u. The velocity in the z-direction is w, which is perpendicular to both u and v.

asymmetric, in general, in clinical practice a Poiseuille profile is assumed and the flow is calculated based on the measured maximum or centerline velocity.[5,6]

The Poiseuille method is adequate for quasistatic flow in straight arteries with axial velocities only. However, most arteries are tapered, curved, and bifurcated, causing the axial velocity distribution to be altered by transversal velocities, resulting in asymmetrical axial velocity profiles and consequently in inaccurate flow estimations.[7] To perform the velocity measurements, the ultrasound beam needs to be positioned, not perpendicular, but at a certain angle with respect to the centerline of the artery (the insonation angle). The uncertainty in this angle influences the error of the Doppler measurement.[8] Another disadvantage is that the motion of the artery wall cannot be measured accurately at the same time since the ultrasound beam needs to be positioned perpendicular to the artery for such a measurement.

To study vascular impedance (transfer function between pressure and the volume flow), it is important to measure simultaneously the pressure and the flow at a specific area of the blood circulation of the patient. Theoretically, the local pressure can be deduced from the wall distension and the pulse wave velocity. A relatively new method to measure axial velocity profiles with ultrasound is a particle imaging velocimetry based ultrasound measurement.[9] The measured (asymmetric) axial velocity profiles are obtained perpendicular to the artery and can be combined with the measurement of wall distension at the same time from the same ultrasound signal. To obtain an accurate combined measurement, a novel method needs to be found to accurately estimate the local volume flow from the measured (asymmetrical) axial velocity profiles at a certain cross section of a curved artery. Therefore, this study will focus on *the effect of curvature on the axial velocity profile for steady flow through a curved tube and a new volume flow estimation method*.

The flow regime of interest is based on the parameters of the carotid artery to obtain physiologically relevant velocity distributions. The mean axial velocity in the common carotid artery is roughly 0.2 m/s, the radius is about 4 mm, and the maximum curvature ratio is about 0.16.[10] It is assumed that blood is a Newtonian fluid with a density of $\rho=1.132\times10^3$ kg m^{-3} and a dynamic viscosity of $\eta=3.56\times10^{-3}$ kg m^{-1} s^{-1}. This results in a Dean number (see Sec. II A for definition) of 580. Therefore, the main region of interest is defined as $1\leq\mathrm{Dn}\leq1000$. The parameters stated above for the density, viscosity, and radius are also used for obtaining the analytical and computational results in this study.

B. Introduction to the theoretical background

Nearly all authors mentioned in Sec. II A of this paper give the same theoretical/physical explanation to describe steady flow in a curved tube. When a fluid flows from a straight tube into a curved tube, a change in the flow direction is imposed on the fluid. The fluid near the axis of the tube has the highest velocity and therefore experiences a larger centrifugal force ($\rho w^2/R$, where w is the axial velocity, ρ is the density, and R is the distance to the center of curve) compared to the fluid near the walls of the tube. Therefore, the fluid at the center of the tube will be forced to the outside of the curve. The fluid near the walls, having a lower axial velocity, on the outer side of the curve will be forced inward along the walls of the tube because the pressure is lower at the inside of the curve. This overall balance between the radial pressure and the centrifugal forces results in a secondary flow, which influences the axial velocity distribution (Fig. 1).

During the past century a few analytical approximation methods were derived to explain and predict the behavior of stationary flow in curved tubes. The solutions obtained by Dean,[11] Topakoglu,[12] and Siggers and Waters[13] will be evaluated more extensively and compared with each other. These authors derived analytical solutions for small Dean numbers ($\mathrm{Dn}\ll1$) and assumed that the analytical solution for a curved tube is just a small disturbance on the Poiseuille flow of a straight tube, with the flow being driven by the pressure gradient.

Topakoglu[12] and Siggers and Waters[13] used the toroidal coordinate system with the coordinates (r,θ,z) (see Fig. 2). Dean[11] used a slightly different definition, but the results as presented in this article are adapted to the coordinate system definition of Topakoglu[12] and Siggers and Waters.[13] The most relevant results to this study obtained by the authors with respect to the axial velocity profiles are briefly shown, together with the equations, which relate the flow in a curved tube to the flow in a straight tube.

C. Outline

The paper is structured as follows. In Sec. II a short theoretical background of literature on steady flow in curved tubes is presented. Three analytical approximation methods for fully developed flow in curved tubes are discussed more extensively. Then a novel estimation method, based on the analytical approximation methods, is derived to assess the volume flow through a curved tube from the axial velocity profiles. Finally, a computational fluid dynamics (CFD) model is introduced, which is applied to investigate flow in curved tubes for ranges of flow rate and curvature ratio, where no analytical solution exists.

In Sec. III axial flow profiles from the analytical approximation methods are compared with each other and with the results of the CFD models so as to validate the analytical approximation methods. Furthermore, the CFD solutions are used to validate the novel volume flow estimation method and to compare the new estimation method with the currently used Poiseuille method. Sections IV and V contain the discussion and the conclusions.

II. METHODS

A. Theoretical background

In 1928 Dean[11] published the derivation of an analytical solution describing the steady flow of an incompressible fluid in curved tubes with a small curvature, $\delta=a/R_0$, where a is the radius of the tube and R_0 is the curvature radius of the tube. This analytical solution was based on the assumption that the secondary flow is just a small disturbance of the Poiseuille flow in a straight tube. He noticed that when the fluid motion is slow, the reduction in flow rate due to the curvature of the tube depends on the single variable K defined by $K=2\mathrm{Re}^2\ a/R_0$, in which the Reynolds number can be defined as $\mathrm{Re}=aW_{\max}/\nu$, where $W_{\max}$ is the maximum velocity in the axial direction and ν is the kinematic viscosity.

Dean[11] derived a series solution expanded in K to describe the fully developed, steady flow analytically in a tube with a small K-number [see Appendix, Sec. 1, which shows the resulting expressions for the axial velocity (w)]. He also derived the ratio of the flow rate through a curved tube in his model (Q_{cD}) to that in a straight tube (Q_{sD}) driven by the same pressure gradient. This ratio equals

$$\frac{Q_{cD}}{Q_{sD}} = 1 - 0.030\ 58\left(\frac{K}{576}\right)^2 + 0.011\ 95\left(\frac{K}{576}\right)^4 + O(K^6). \tag{1}$$

Dean[11] stated that this equation predicts the flow fairly accurate for $K<576$. When $K=576$, a reduction in flow rate is calculated of approximately 1.9%, compared to flow in a straight tube.

The second approximation method was derived by Topakoglu.[12] A power series expansion is performed in δ to find the solution for the set of nonlinear differential equations he derived (see Appendix, Sec. 2). He obtained the following relation for the normalized flow rate through the curved tube in comparison with flow through a straight tube, under the same conditions:

$$\frac{Q_{cT}}{Q_{sT}} = 1 - \frac{1}{48}\delta^2\left(\frac{1.541}{67.2}n^2 + 1.1n - 1\right) + O(n^3), \tag{2}$$

where $n=(\mathrm{Re}/6)^2$.

In 1968, McConalogue and Srivastava[14] made an extension to the work of Dean. They solved the equations numerically with Fourier series for $96<\mathrm{Dn}<600$. The Dean number is defined as

$$\mathrm{Dn} = 4\mathrm{Re}\left(\frac{2a}{R}\right)^{1/2} = \sqrt{\left(\frac{2a^3}{\nu^2 L}\right)\frac{G_{\mathrm{MS}}a^2}{\mu}}, \tag{3}$$

where G_{MS} is the mean pressure gradient, ν is the kinematic viscosity, and μ is the dynamic viscosity coefficient. The Dean number is based on the K-number proposed by Dean, with $\mathrm{Dn}=4\sqrt{K}$ and so a Dean number of 96 corresponds to a K-number of 576.

McConalogue and Srivastava[14] showed that for $\mathrm{Dn}=600$, the position of the maximum axial velocity is reached at a distance less than 0.38 times the radius from the outer boundary and that the flow is reduced by 28% in comparison to a straight tube. Collins and Dennis[15] obtained numerical solutions for an extended range of Dean numbers, $96<\mathrm{Dn}<5000$. They gave the contour plots of the axial and transversal velocities for Dn=96, 500, 605.72, 2000, and 5000, which show a good agreement with the results of McConalogue and Srivastava[14] for Dn=96 and Dn=605.72.

The most recent publication of relevance to this study is the article of Siggers and Waters.[13] To derive an analytical approximation method for flow in curved tubes with a small Dean number and small curvature ratio, Siggers and Waters[13] used the series solution for w expanded in Dn, where w_k is allowed to depend on δ (see Appendix, Sec. 3).

Siggers and Waters[13] calculated the axial flow rate in a curved tube driven by the axial pressure gradient $-(\rho\nu^2 G_{\mathrm{SW}}/a^3)$ with $G_{\mathrm{SW}}=4\mathrm{Re}$, which is according to their calculations given by

$$Q_{c\mathrm{SW}} = \pi\ \mathrm{Dn}\left(\frac{1}{8} + \frac{1}{2^7\times 3}\delta^2 - \frac{11}{2^{15}\times 3^3\times 5}\mathrm{Dn}^2\delta - \frac{1541}{2^{28}\times 3^6\times 5^2\times 7}\mathrm{Dn}^4 + O(\delta^4, \mathrm{Dn}^2\delta^3, \ldots)\right). \tag{4}$$

To obtain the flow ratio, this equation should be divided by the corresponding flow in a straight tube (Q_s) and the dimensional flow rate is $a\nu Q_{c\mathrm{SW}}/\sqrt{2\delta}$.

A summary of the three analytical approximation methods discussed above is shown in Table I. In each method a slightly different series expansion method was used and an equation to describe the flow in a curved tube compared to the flow in a straight tube was derived. More extensive overviews about earlier work on flow in curved tubes are given by Pedley,[16] Ward-Smith,[17] and Berger and Talbot.[18]

TABLE I. Overview of the series expansions used by the authors to derive their analytical approximations.

Author	Series expansion to:	Flow ratio $Q_c/Q_s=$
Dean (1928)	$K=2\mathrm{Re}^2\delta=\frac{\mathrm{Dn}^2}{16}$	$1-0.030\,58\left(\frac{K}{576}\right)^2+0.011\,95\left(\frac{K}{576}\right)^4$
Topakoglu	δ	$1-\frac{1}{48}\delta^2\left(\frac{1.541}{67.2}n^2+1.1n-1\right)$
Siggers and Waters	Dn and δ	$\frac{\pi\ \mathrm{Dn}}{Q_s}\left(\frac{1}{8}+\frac{1}{2^7\times 3}\delta^2-\frac{11}{2^{15}\times 3^3\times 5}\mathrm{Dn}^2\delta-\frac{1541}{2^{28}\times 3^6\times 5^2\times 7}\mathrm{Dn}^4\right)$

B. Flow estimation methods

In clinical practice the volume flow is estimated by assessment of the maximum axial velocity, obtained with Doppler ultrasound, and the assumption of a Poiseuille velocity distribution across the artery. However, the axial velocity profiles of curved arteries become more and more asymmetrical for increasing flow rates (Re) and increasing curvature ratios (δ). When the volume flow is estimated based on the maximum velocity, the asymmetry of the velocity profiles is neglected, causing an error in the volume flow estimation. Therefore, a new volume flow estimation method, which can be applied in clinical practice, is investigated and compared with the flow calculations resulting from the Poiseuille method.

Motivated by the analytical solutions for the axial velocities derived by Dean,[11] Topakoglu,[12] and Siggers and Waters[13] (see Appendix), we propose a new method to estimate the flow rate from the velocity profile on a diameter, which we call the "cos θ-method." The cross section is divided into two semicircles along the diameter perpendicular to that on which the measurement is taken. The flow rate ($Q_{\cos\theta}$) is estimated by assuming the axial flow to be axisymmetric in each semicircle, giving the expression

$$Q_{\cos\theta}=\pi\int_0^a rw^+(r)dr+\pi\int_0^a rw^-(r)dr, \tag{5}$$

where a is the tube radius, and $w^+(r)$ and $w^-(r)$ are the measured velocities on the two radii (see Fig. 3).

We expect this method to produce more accurate results than the Poiseuille method since each of the three aforementioned analytical approximations shows that the largest correction to Poiseuille flow in the axial velocity profile takes the form $f(r)\cos\theta$ for some function f. It can be shown that this correction does not contribute to either the true flux or to the estimate given by the cos θ-method; hence any errors will be given by smaller terms. Conversely, such a term would affect the error in the Poiseuille method, leading to less accurate results.

It should be mentioned that the cos θ-method is, in principle, applicable for every arbitrary angle of measurement through the tube, as long as the diameter along which the measurement is performed, crosses the center point. However, in clinical practice the ultrasound beam may not always measure along the true diameter of the artery.

In Sec. III the (asymmetric) axial velocity profiles calculated with the CFD model (see Sec. II C) are used as input for the Poiseuille method and the cos θ-method; the imposed flow is used as a reference value.

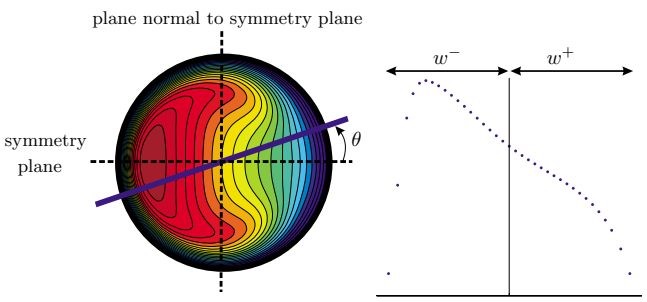

FIG. 3. (Color online) Visual explanation of the division of the axial velocity profile into w^+ and w^-. In this figure the symmetry plane and the plane normal to the symmetry plane of the curved tube are indicated.

C. CFD

The aim of the CFD simulations is to calculate the axial velocity distribution of steady, fully developed flow in curved tubes. The results will be used to validate the range of applicability of the analytical approximation methods and to investigate the flow in curved tubes at higher Dean numbers, for which the analytical approximation methods are invalid, but which are most relevant for large arteries in humans.

It is assumed that the fluid in the curved tube is an incompressible, Newtonian fluid, which is steady. The governing equations are

$$\nabla\cdot\boldsymbol{v}=0,\quad \rho\frac{\delta\boldsymbol{v}}{\delta t}+\rho\boldsymbol{v}\cdot\nabla\boldsymbol{v}=-\nabla p+\eta\nabla^2\boldsymbol{v}.$$

Here the gravity and body forces are neglected, $\boldsymbol{v}$ is the velocity, p is the pressure, ρ is the fluid density, and η is the dynamic viscosity. At the tube walls no-slip boundary conditions are applied and at the inlet a flow rate is prescribed.

The mesh of the finite element based CFD model is composed of isoparametric hexahedral volume elements with 27 points. The elements are of the triquadratic hexahedron Crouzeix–Raviart type, with a discontinuous pressure over the element boundaries. An integrated or coupled approach is used for the continuity equation.[19] For the temporal evolution, a first order Euler-implicit discretization scheme is applied. To linearize the convective term, the Newton–Raphson method is chosen. The Bi-CGstab iterative solution method,

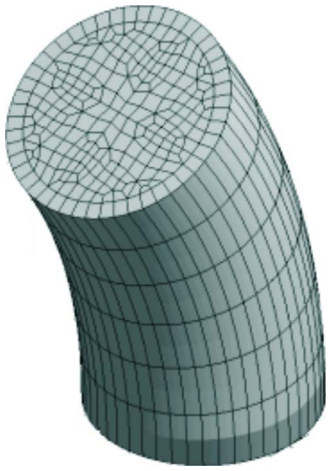

FIG. 4. (Color online) The mesh of the CFD model with a curvature ratio of δ=0.16.

with an incomplete LU-decomposition preconditioner, was applied to solve the linearized set of equations.

A CFD curved tube model for fully developed flow is implemented in the finite element package SEPRAN.[20] The mesh of the CFD model consists of a small curved section of 6 axial elements, with a total length of 4 times the radius. It has 18 elements across the diameter and 48 elements along its circumference (see Fig. 4).

Initially, a Poiseuille velocity distribution is prescribed at the inlet,

$$w(r) = W_{\max}\left[1 - \left(\frac{r}{a}\right)^2\right]. \tag{6}$$

For the subsequent time steps, the velocity distribution is taken at the plane halfway up the tube; this velocity distribution is multiplied with a rotation matrix in order to correct for the curvature, before it is prescribed at the inlet of the next time step. It is found that the velocity distribution in the midplane is not influenced by the stress free outlet condition. For representative Dean numbers the fully developed curved tube flow obtained with this method was compared to simulations performed with a longer tube, which had a length of 80 times the radius and was long enough to obtain a fully developed curved tube flow by only prescribing a Poiseuille inlet flow. A difference of 0.2% was found, whereas a 50-fold reduction in computation time was achieved using the former method.

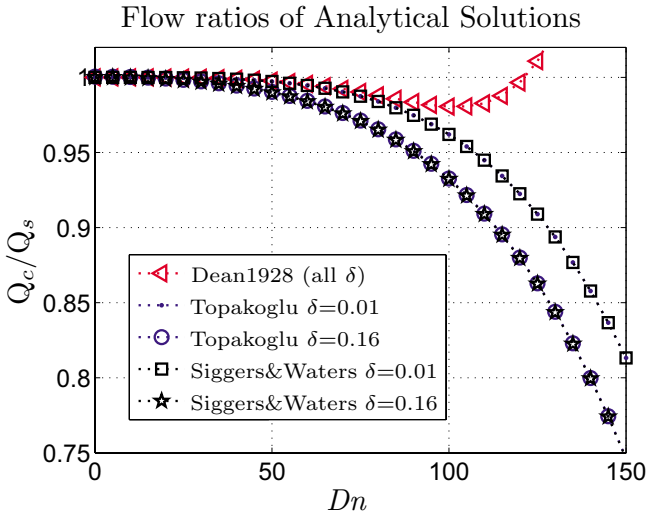

FIG. 5. (Color online) The flow ratios between flow in a curved tube (Q_c) and flow in a straight tube (Q_s) of the analytical approximations derived by Dean, Topakoglu, and Siggers and Waters.

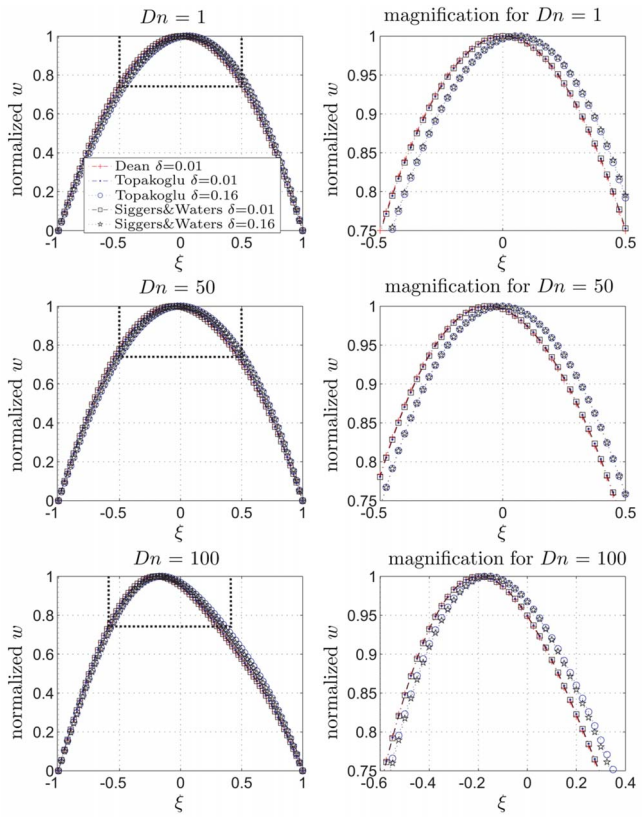

FIG. 6. (Color online) The normalized axial velocity profiles of the analytical approximations derived by Dean (Ref. 11), Topakoglu (Ref. 12), and Siggers and Waters (Ref. 13) for Dn=1, 50, and 100 and δ=0.01 or 0.16. The right panels depict magnifications of the central region. The velocity profiles derived by Dean do not change for different δ's for a fixed Dean number, therefore, only δ=0.01 is shown. The axial velocity profiles with δ=0.01 are laying on top of each other for every Dean number, while the velocity profiles of Topakoglu and Siggers and Waters for δ=0.16 are shifted to the right.

The simulations are performed for all combinations of Dn=1, 10, 25, 50, 100, 200, 400, 600, 800, and 1000 with δ=0.01, 0.02, 0.04, 0.08, 0.10, or 0.16, except Dn=1000 and δ=0.01 due to computational instabilities. For the simulations it is assumed that blood is a Newtonian fluid with a density of $\rho = 1.132 \times 10^3$ kg m^{-3} and a dynamic viscosity of $\eta = 3.56 \times 10^{-3}$ kg m^{-1} s^{-1} (see also Sec. I A). In Sec. III the axial velocity profiles will be analyzed and compared with analytical and computational results obtained from the literature.

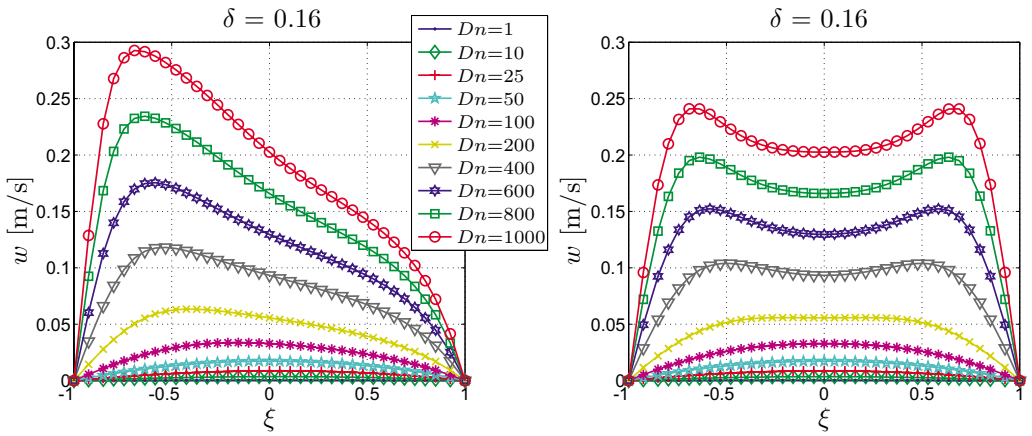

FIG. 7. (Color online) The axial velocity profiles for different Dean numbers of δ=0.16: in the left figure the normalized velocity profiles for the symmetry plane and in the right figure the normalized velocity profiles for the plane normal to the symmetry plane.

III. RESULTS

A. Analytical approximation methods

Dean,[11] Topakoglu,[12] and Siggers and Waters[13] derived analytical approximations by using series expansion (see Table I) to solve the Navier–Stokes equations with the assumption that $\delta \ll 1$ and $K \ll 1$ or $\mathrm{Dn} \ll 1$. The authors all used a different scaling method, which were not always explicitly stated. Therefore, the results of this study are normalized to perform a comparison between the three different analytical approximation methods. The axial velocity profiles are divided by the maximum of their axial velocity. The velocity profiles are given as a function of ξ, with $\xi = r/a$ going from -1 to 1 (so the half of the measurement diameter in the $-90° < \theta \leq 90°$ plane is defined positive and the other half in the $90° < \theta \leq 270°$ plane is defined negative).

The Q_c/Q_s flow ratios of the analytical approximation methods are plotted in Fig. 5. The solution derived by Dean[11] only depends on K, so if K (or Dn) does not change, the solution will not change for different curvature ratios. The solutions of Topakoglu[12] and Siggers and Waters[13] do change for different curvature ratios, while the Dean number stays the same. Around Dn=60, Dean's solution starts to deviate from the other solutions, it even increases for $\mathrm{Dn} > 100$. The flow ratios derived by Topakoglu[12] and Siggers and Waters[13] give nearly the same result. They keep on decreasing and become negative for $\mathrm{Dn} > 220$ (not visible in Fig. 5).

Figure 6 shows the normalized axial velocity profiles in the plane of symmetry derived by the three analytical solutions for Dn=1, 50, 100 and δ=0.01, 0.16 based on the equations for the axial velocities as given in the Appendix. As Dn increases, the position—where the maximal velocity is achieved—moves toward the outside of the curve, while as δ increases, this position moves to the inside of the curve; this effect is supported by the analytical solutions of Topakoglu[12] and Siggers and Waters.[13] For example, if δ=0.16, then as long as $\mathrm{Dn} < 50$, the maximum velocity is achieved at a positive value of ξ (closer to the inside of the curve).

B. CFD

Results obtained with the CFD model for all simulations performed with a curvature ratio of δ=0.16 are shown in Fig. 7. The position of the maximum velocity can be determined from the axial velocity profiles of the symmetry plane. For a higher Dean number and so a higher Reynolds number, the position of the maximum velocity shifts more to the outside of the curve, which is in accordance to the derived analytical solutions of Dean,[11] Topakoglu,[12] and Siggers and Waters.[13]

The position of the maximum velocity as function of the

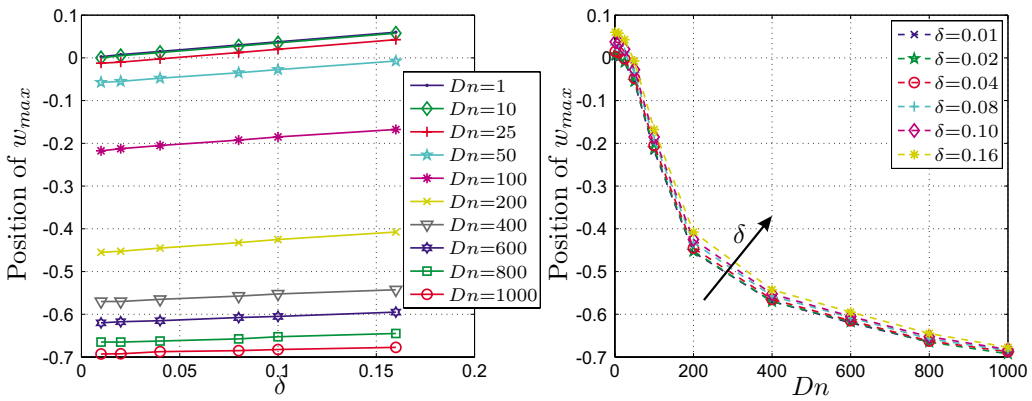

FIG. 8. (Color online) The position of the maximum velocity as function of δ for different Dean numbers on the left and on the right as function of Dean number for different curvature ratios.

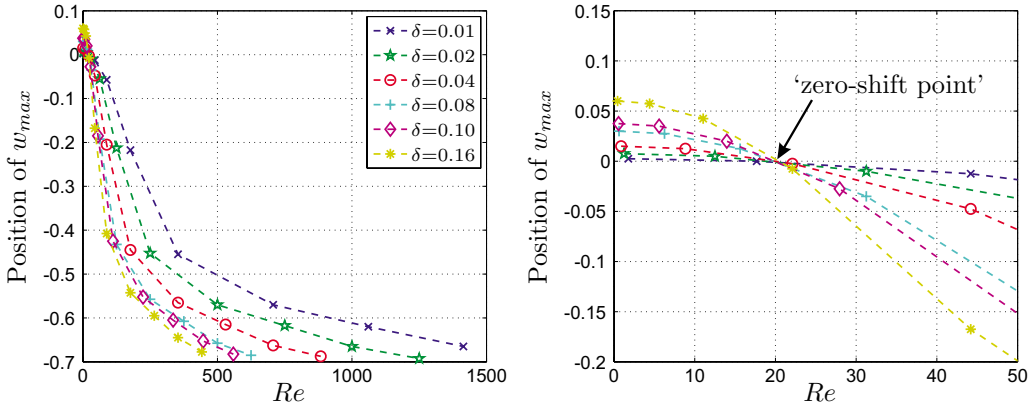

FIG. 9. (Color online) The position of the maximum velocity (w_{max}) as function of Reynolds number for different δ, with, on the right, a magnification of the zero-shift point around Re=20.

Dean number and the curvature ratio is shown in Fig. 8. It shows that the position of the maximum velocity as function of the curvature ratio (δ, left graph) or as function of the Dn number (right graph) have different relations. There seems to be a linear relation between the position of the maximum and δ, but this linear relation is not the same for different Dean numbers.

The right graph in Fig. 8 shows that for low Dean numbers the position of the maximum velocity shifts to the inside of the curve. From Dn=50 and higher, the position of the maximum velocity is always shifted to the outside of the curve. For increasing Dean numbers, the shift increases. The differences in the position of the maximum velocity for different curvature ratios but with the same Dean number become less for higher Dean numbers.

The position of the maximum axial velocity as function of Reynolds number is shown in Fig. 9. Around Re=20 all curves pass through the symmetry point (zero), which from now on is called "zero-shift point." For smaller Reynolds numbers, the position of the maximum is shifted to the inside of the curve and for higher Reynolds numbers, the position is shifted to the outside of the curve.

C. CFD versus analytical approximation methods

The results of the analytical approximation methods and the CFD simulations can be compared by their normalized axial velocity profiles. The analytical solution derived by Siggers and Waters[13] is compared to the profiles calculated with the CFD model in Fig. 10. These graphs show that the analytical solutions are similar to the CFD simulations for $\mathrm{Dn} \leq 50$ and $0.01 \leq \delta \leq 0.16$. For Dn=100, the analytical approximation deviates from the axial velocity profile derived with the CFD model. This deviation increases for higher Dean numbers. The same results will be obtained for the axial velocity profiles calculated from the analytical approximation method of Topakoglu,[12] as his method gives nearly the same results as the approximation method of Siggers and Waters.[13] The analytical approximation method of Dean[11] agrees with the other analytical solution methods for δ=0.01, as this value is closest to δ=0, for which the analytical solution was derived.

Siggers and Waters[13] derived their analytical approximation for curved tubes using series expansion and by assuming that $\mathrm{Dn} \ll 1$ and $\delta \ll 1$. The relative position of the maximum velocity $r_{W\,\max}$ is related to the Dean number and curvature ratio by

$$r_{W\,\max} = \frac{19\ \mathrm{Dn}^2}{2^{14} \times 3^2 \times 5} - \frac{3\delta}{8} + O(\delta^3, \mathrm{Dn}^2\delta^2, \mathrm{Dn}^4\delta, \mathrm{Dn}^6). \tag{7}$$

Figure 11 shows this relative position as function of Dean number for different values of δ in comparison with the results obtained with the CFD model (see also Fig. 8). In the

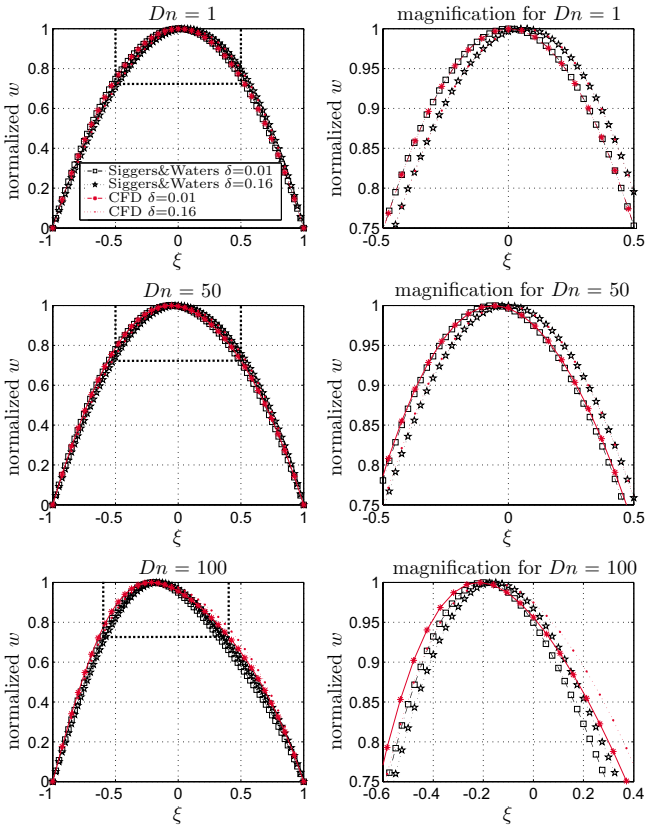

FIG. 10. (Color online) The normalized axial velocity profiles of the analytical solution derived by Siggers and Waters (Ref. 13) vs the results of the infinite tube simulation for Dn=1, 50, or 100 and δ=0.01 or 0.16.

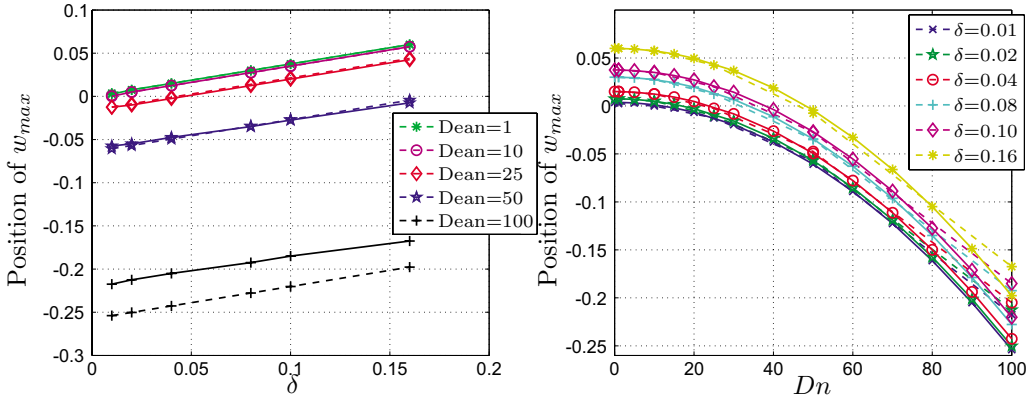

FIG. 11. (Color online) Comparison of the results of the CFD simulations (dotted line) and the analytical approximation derived function of Siggers and Waters (Ref. 13) (solid line). At the left, the position of the maximum velocity is plotted as function of the curvature ratio for different Dean numbers. The right graph shows the position of the maximum velocity as function of Dean number for different curvature ratios. The solutions for Dn=1, 10 are very close, while a little difference can be seen for Dn=25, 50 and for Dn=100 the solutions of the CFD are distinct from the analytical approximation.

left graph the position of the maximum velocity as function of δ is given for both methods and in the right graph as function of the Dean number. Again the results of the analytical approximation coincide with the CFD results for Dn $\leq$50, while for higher Dn numbers the analytical solutions starts to deviate from the CFD results.

D. Flow estimation methods

The axial velocity profiles obtained with the CFD model are used as input to compare the volume estimation methods with each other and with the imposed flow. The flow estimation based on the cos θ-method is performed on the axial velocity profiles of the symmetry plane and the plane normal to the symmetry plane (see Fig. 3). The deviation of the estimated flow from the imposed flow for the different flow estimation methods is shown in Fig. 12 for simulations with δ=0.01 and δ=0.16.

The results in Fig. 12 show that the cos θ-method and the Poiseuille method give similar results for Dn$\leq$100. For higher Dean numbers, the Poiseuille method shows a consistent underestimation of the volume flow, which is nearly three times larger than the underestimation of the cos θ-method for high Dean numbers (Dn$>$400). The cos θ-method with the plane normal to the symmetry plane as input results in an overestimation of the flow for higher Dean numbers.

The deviation of the calculated flow of the cos θ-method based on profiles in the symmetry plane is compared to the imposed volume flow for different Dean numbers and curvature ratios (see Fig. 13).

For a curvature ratio of δ=0.01 and 1$\leq$Dn$\leq$800, the cos θ-method based on the axial velocity profile in the symmetry plane has a maximum deviation from the imposed flow of less than 4%, while the Poiseuille method has a maximum deviation of 12.7%. The cos θ-method based on the axial velocity profile in the plane normal to the symmetry plane results in a maximum deviation of 6.4%,

A curvature ratio of δ=0.16 and 1$\leq$Dn$\leq$200 gives similar results for the cos θ-method based on the axial velocity profiles of both the symmetry and its normal plane. For higher Dean numbers the cos θ-method based on the symmetry plane gives an underestimation of the flow, which is maximally 5.5% at Dn=600. The cos θ-method based on the plane normal to the symmetry plane gives an overestimation

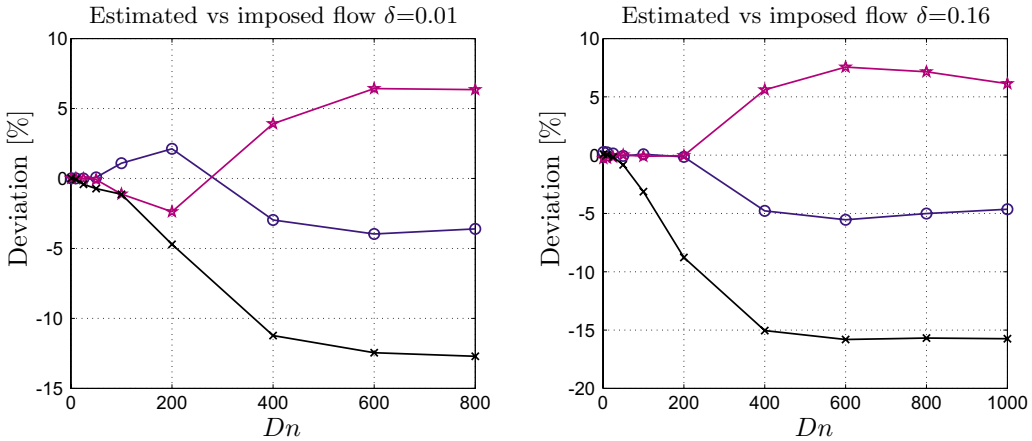

FIG. 12. (Color online) The deviation of the estimated volume flow from the imposed volume flow for δ=0.01 (left figure) and δ=0.16 (right figure) as function of Dean number. The estimated flow is based on the cos θ-method applied to the a velocity measurement along the symmetry plane (-○-) or the plane normal to the symmetry plane (-⋆-) or the Poiseuille method applied to the symmetry plane (-×-).

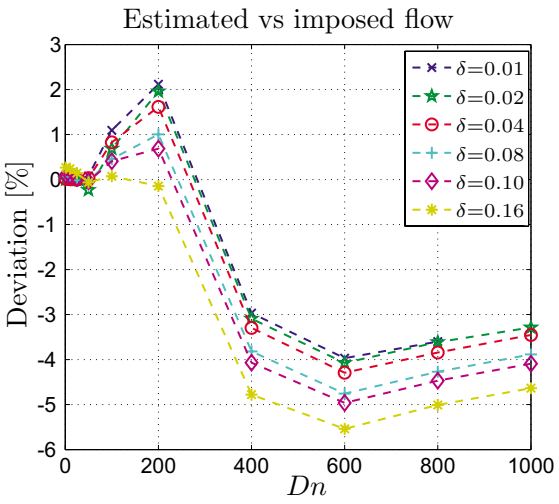

FIG. 13. (Color online) The deviation of the estimated volume flow (based on the cos θ-method) compared to the calculated flow in percentages for different curvatures, based on velocity profiles obtained from the symmetry plane.

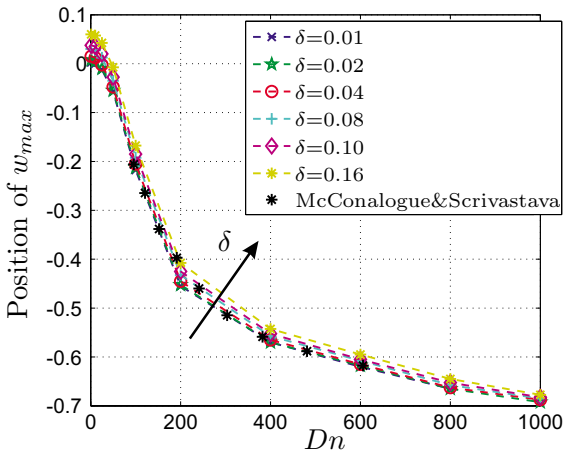

FIG. 14. (Color online) The position of the maximum velocity as function of Dean number for different δ's with the results of McConalogue and Srivastava (Ref. 14).

of the flow which is maximally 7.5% at Dn=600. The Poiseuille method gives a consistent underestimation for Dn>50, which is maximally 15.8%.

Figure 13 shows that for the different curvatures the deviation of the cos θ-method is maximally 5.5% and is reached for all curvatures around Dn=600, for higher Dean numbers, the deviation decreases. For small Dean numbers ($1 \leq Dn \leq 25$), the higher curvature ratios give a slightly larger error, while for intermediate Dean numbers ($25 \leq Dn \leq 200$), the smaller curvature ratios result in larger deviations from the imposed flow. Finally for high Dean numbers ($400 \leq Dn \leq 1000$) the largest curvature ratios have the largest deviation.

IV. DISCUSSION

A. Analytical approximation methods

All analytical approximation methods are derived for Dn or $K \ll 1$ and $\delta \ll 1$; however, the results are accurate for $Dn \leq 50$. The equations derived for the flow ratios, which compare flow in a curved tube to flow in a straight tube with the same pressure gradient, already show that Dean's analytical solution does not depend on δ for a constant K or Dn. His solution becomes unrealistic at smaller Dean numbers, compared to the solutions of Topakoglu[12] and Siggers and Waters,[13] the flow ratio increases for Dn>100. The analytical approximation methods derived by Topakoglu[12] and Siggers and Waters[13] depend on the curvature ratio and give similar results.

Investigation of the axial velocity profiles results in essentially the same observations. The three approximation methods give the same results for δ=0.01. An interesting effect is the displacement of the maximum velocity to the inside of the curve for higher curvature ratios of the analytical solutions derived by Topakoglu and Siggers and Waters. Topakoglu[12] did not mention this effect in his paper. Siggers and Waters[13] did notice that their equation for w_{01} causes the maximum velocity to move toward the inside of the curve for increasing δ, but did not give any physical explanation.

B. CFD

The fully developed flow profiles calculated with the CFD tube model correspond with results from the literature.[14,15] However, it is difficult to compare the results exactly. Often only the Dean number is given in combination with the value of the (scaled) maximum axial velocity, but nothing is known about the exact values for the curvature ratio, diameter, viscosity parameters, etc. A complete description of a flow problem in a curved tube requires two of the characteristic dimensionless numbers δ, Re and Dn, to be stated.

Most research is focused on the flow ratio of flow through a straight tube in comparison with flow in a curved tube driven by the same pressure gradient. For the simulations in this study, flow is prescribed and no attention has been paid to the pressure gradient since this cannot be assessed by ultrasound measurements.

Besides a qualitative comparison between the contour plots of the axial velocities, another more quantitative comparison can be made by observing the position of the maximum velocity. McConalogue and Srivastava[14] used a Fourier-series development method to solve the momentum and continuity equation in the toroidal system numerically. They published their resulting contour plots of the axial velocity for different values of Dean number between Dn=96 and Dn=605.72. From these contour plots the relative position of the maximum velocity can be deduced.

In Fig. 14 the results are shown in the same graph as the maximum positions computed with the CFD model. The figure shows a good resemblance between the results from McConalogue and Srivastava and the results of the CFD model. As McConalogue and Srivastava[14] stated that they assume δ to be small, one should expect their results should agree most closely with the δ=0.01 solutions of the simula-

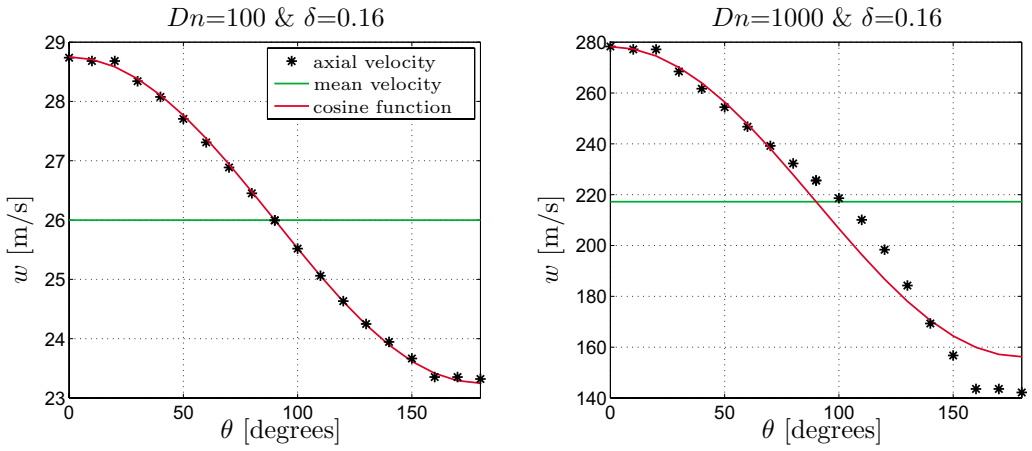

FIG. 15. (Color online) The axial velocity for a fixed radius, $r=2$ mm, as function of the angle (θ) with on the left Dn=100 and $\delta=0.16$ and on the right Dn=1000 and $\delta=0.16$.

tions. As can be seen in Fig. 14 their results do match the $\delta=0.01$ results closely, except two data points around Dn=200.

C. CFD versus analytical approximation methods

Comparison of the analytical axial velocity profiles with the calculated profiles of the CFD simulations shows that the analytical solution predicts the axial velocity very well for $\mathrm{Dn}\leq 50$. It is striking that, despite the assumptions made for the approximation (small δ), the analytical solution also coincides very well with the results of the CFD model for higher curvature ratios, up to $\delta=0.16$. Furthermore, the equation for the position of the maximum velocity derived by Siggers and Waters[13] coincides very well for $\mathrm{Dn}\leq 50$ with the calculated positions of the CFD model.

The computational method presented in this study and the analytical method of Siggers and Waters[13] both predict that for low Dean numbers the maximum position is shifted to the inside of the curve. This effect increases for an increasing curvature ratio. Since the velocity profiles are fully developed in space and time, the shift to the inside of the curve cannot be explained by entrance effects, which holds for frictionless flow in the core of the tube.[10,21]

A possible explanation could be that for low Dean numbers, and especially for low Dean numbers with a larger curvature ratio, the Reynolds number is low. Then the values of the velocity in the secondary field are small, which results in a negligible pressure gradient in the radial direction which becomes comparable to the pressure distribution in a straight tube. However, the geometry of the tube is still curved; therefore the fluid velocity will be maximal at the inside of the tube. There the fluid is subject to the highest pressure gradient in the axial direction because of the shortest axial distance. This implies that the shift to the inside of the tube is a pure geometry driven effect.

The shift of the maximum velocity to the inside of the curve for lower Dean numbers was noticed earlier by Murata *et al.*,[22] but not many other authors mention this phenomenon. Murata *et al.*[22] did not investigate this effect for different curvature ratios and Reynolds numbers.

Plotting the relative position of the maximum velocity as function of the Reynolds number shows a zero-shift point, as we would like to call it (see Fig. 9). Around $\mathrm{Re}\approx 20$ the effect caused by the axial pressure difference balances the effect of the centrifugal forces (radial pressure difference). This zero-shift point can also be found by inserting $r_{W\,\max}=0$ in the equation derived by Siggers and Waters,[13] which results in two solutions. The first solution is $\delta=0$, which corresponds to a straight tube, and the second solution is Re=21.3, which corresponds to the zero-shift point.

D. Flow estimation methods

The Poiseuille method and the cos θ-method give similar results for $\mathrm{Dn}\leq 100$. For higher Dean numbers, the Poiseuille method becomes more and more inaccurate, with an estimation error of 12.7% compared to the imposed flow for Dn=1000 and $\delta=0.01$. The cos θ-method gives much better results and deviates maximally 4% from the imposed flow. The cos θ-method based on the axial velocity profile in the plane perpendicular to the plane of symmetry results in a maximum deviation of 6.4%. The results for a curvature ration of 0.16 give similar results, but all deviations are slightly elevated.

The cos θ-method is investigated for different curvature ratios (see Fig. 13), and the maximal deviation in the symmetry plane is only 5.5%, which is a much better estimation than the Poiseuille method. The analytical approximation methods support the cos θ-method because all derived methods show that the first correction term on the Poiseuille component of the axial velocity depends on $\cos(\theta)$, for a fixed r. To investigate whether the analytical solutions are right, the axial velocity (obtained from the CFD simulations) is plotted as function of a fixed r, $r=2$ mm, for Dn=100 and $\delta=0.16$ (Fig. 15). This figure shows that the axial velocity as function of θ for a fixed r can be described with a cosine function, which is plotted in the figure based on the mean axial velocity and the amplitude at $\theta=0$.

As shown earlier, the analytical approximation methods are valid for $\mathrm{Dn}<100$. So the error of the cos θ-method can

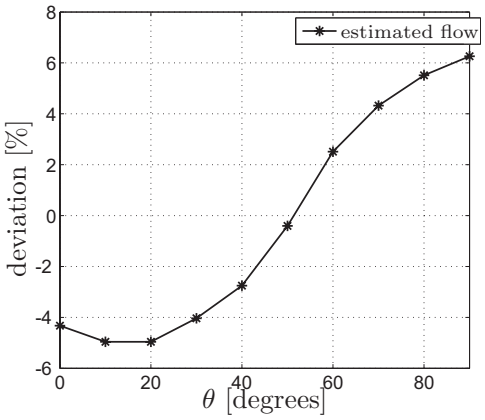

FIG. 16. The deviation of the estimated volume flow from the imposed flow for different angles with respect to the symmetry plane of the simulation with Dn=1000 and δ=0.16.

be caused by an asymmetric, multiharmonic change in the axial velocity in curved tubes for higher Dean numbers. Therefore, the axial velocity is plotted as function of a fixed r, r=2 mm, for Dn=1000 and δ=0.16 (see right graph in Fig. 15). From this result, it is clear that for this case a single cosine function cannot approximate the axial velocity as a function of θ for a fixed r anymore.

In clinical practice, the axial velocity profile will not, in general, be measured exactly on the symmetry plane. Therefore the influence of the angle of the ultrasound beam with respect to the tube is investigated by estimating the flow of the axial velocity profiles obtained under a certain angle with respect to the symmetry plane (see Fig. 16). This indicates that for Dn=1000 and δ=0.16, the maximum error depending on the angle is an overestimation of volume flow calculation by 6.1%, which is obtained at the plane normal to the symmetry plane (θ=90°).

V. CONCLUSIONS

The analytical approximation methods for flow in curved tubes derived by Dean,[11] Topakoglu,[12] and Siggers and Waters[13] were investigated, and a quantitative comparison has been made. The results show that the analytical approximation derived by Dean does not depend on the curvature ratio for a fixed Dean number, while the solutions of Topakoglu and Siggers and Waters do. The solutions derived by Topakoglu and Siggers and Waters give similar results.

A CFD model for fully developed curved tube flow was developed to simulate the axial velocity in a curved tube and simulations were performed in the ranges of $1 \leq \mathrm{Dn} \leq 1000$ and $0.01 \leq \delta \leq 0.16$. The axial velocity profiles obtained with the CFD model are in good agreement with results presented in literature, although it is sometimes hard to compare the results exactly with each other.[14,15]

The analytical approximation methods were compared to the results of the CFD model. The approximations derived by Topakoglu[12] and Siggers and Waters[13] predict the velocity profiles very well for $\mathrm{Dn} \leq 50$ and fair for $\mathrm{Dn} \leq 100$ and all curvature ratios, while Dean's approximation only coincides with δ=0.01. For higher Dean numbers (Dn>100) no proper analytical approximation method exists.

At lower Dean numbers, the position of the maximum velocity is shifted to the inside of the curve, while at higher Dean numbers, the position of the maximum velocity is located at the outside of the curve. This phenomenon can be explained by the relatively low pressure gradient in the radial direction in comparison to the axial pressure gradient, causing the fluid to follow the path with the highest axial pressure gradient, which is at the inner curve at low flow rates.

A zero-shift point is found when the relative position of the maximum velocity, obtained from the CFD simulations, is plotted as a function of the Reynolds number. The equation for the position of the maximum velocity derived by Siggers and Waters[13] was used to derive the exact zero-shift point, which is at Re=21.3. At this point the effect caused by the axial pressure difference equals the effect of the centrifugal forces (radial pressure gradient).

The cos θ-method is supported by the analytical approximation methods. For $\mathrm{Dn} \leq 100$ the Poiseuille method is still sufficient, but for $\mathrm{Dn} \geq 100$ the cos θ-method estimates the volume flow nearly three times better than the Poiseuille method, for δ=0.01 4% versus 12.7%. The axial velocity profile measured at a certain angle from the symmetry plane results in an estimation error of at most 6.2% for Dn=1000 and δ=0.16.

These results indicate that it is possible to estimate the volume flow through a curved tube from a given (asymmetrical) axial velocity profile with the cos θ-method, with a reasonable accuracy. Before this method can be used in clinical practice, the cos θ-method needs to be tested on unsteady flows, non-Newtonian fluids, and finally on axial velocity profiles obtained from patients or volunteers. It should be kept in mind that in most arteries the flow is not fully developed. However, if entrance effects have the same cos θ dependent effect on the axial velocity, this will not give additional errors for the flow estimation with the cos θ-method.

APPENDIX: ANALYTICAL SOLUTIONS FOR THE AXIAL VELOCITY (w)

In this section the results of the analytical approximation methods of Dean,[11] Topakoglu,[12] and Siggers and Waters[13] with respect to the axial velocity (w) are shown. It should be noticed that all authors used different scaling and nondimensionalization methods, which are not explicitly stated here and for which we would like to refer to the corresponding articles.

1. Derivation by Dean

Dean[11] derived a higher order series solution expanded in K to describe the fully developed, steady flow analytically in a tube with a small K-number, which results for the axial velocity in

$$w = w_0 + Kw_1 + K^2 w_2 + \cdots . \tag{A1}$$

The solutions obtained from the series expansion are given by

$$w_0 = 1 - r'^2, \tag{A2}$$

$$w_1 = \frac{\cos\theta}{576}\left(\frac{19r'}{40} - r'^3 + \frac{3r'^5}{4} - \frac{r'^7}{4} + \frac{r'^9}{40}\right), \tag{A3}$$

where $r' = r/a$.

2. Derivation by Topakoglu

Topakoglu[12] performed a power series expansion in δ and by insertion of

$$w = w_0 + \delta w_1 + \delta^2 w_2 + \cdots. \tag{A4}$$

Topakoglu derived the following equations, describing the axial velocity:

$$w_0 = f_0 = \mathrm{Re}(1 - r'^2) \tag{A5}$$

and

$$w_1 = f_1 \cos\theta, \tag{A6}$$

where

$$f_1 = -\tfrac{3}{4} f_0\left[1 - \tfrac{1}{8640}\mathrm{Re}^2(19 - 21r'^2 + 9r'^4 + r'^6)\right]r' \tag{A7}$$

and finally

$$w_2 = f_{20} + f_{22}\cos 2\theta, \tag{A8}$$

where

$$f_{20} = \tfrac{-1}{32} f_0\left\{3 - 11r'^2 + \tfrac{1}{7200}\mathrm{Re}^2\left[148 + 43r'^2 - 132r'^4 + 68r'^6 - 7r'^8 + \tfrac{1}{3225.6}\mathrm{Re}^2(823.8 - 3432.2r'^2 + 5835.8r'^4 - 5252.2r'^6 + 2713.8r'^8 - 803r'^{10} + 121r'^{12} - 7r'^{14})\right]\right\} \tag{A9}$$

and

$$f_{22} = \tfrac{1}{8}\left\{2.5 - \tfrac{1}{3456}\mathrm{Re}^2\left[46.3 - 61.3r'^2 + 29.6r'^4 - 4r'^6 - \tfrac{1}{42\,336}\mathrm{Re}^2(1456.9 - 2402.06r'^2 + 1746.49r'^4 - 705.47r'^6 + 191.23r'^8 - 28.01r'^{10} + 1.6r'^{12})\right]\right\}r'^2. \tag{A10}$$

3. Derivation by Siggers and Waters

Siggers and Waters[13] used a series solution for w expanded in Dn, where w_k is allowed to depend on δ to derive a solution for the axial velocity

$$w = \mathrm{Dn}\sum_{k=0}^{\infty} \mathrm{Dn}^{2k} w_k, \tag{A11}$$

with

$$w_k = \sum_{j=0}^{\infty} \delta^j w_{kj} = w_{k0} + \delta w_{k1} + \delta^2 w_{k2} + \cdots, \tag{A12}$$

with

$$w_{00} = \tfrac{1}{4}(1 - r'^2), \tag{A13}$$

$$w_{01} = -\tfrac{3}{16} r'(1 - r'^2)\cos\theta, \tag{A14}$$

$$w_{02} = \tfrac{1}{128}(1 - r'^2)(-3 + 11r'^2 + 10r'^2\cos 2\theta). \tag{A15}$$

To get the $O(\mathrm{Dn}^3)$ solution they set $w_1 = w_1^{[1]} + w_1^{[2]}$, with $w_1^{[1]} = w_{10}^{[1]} + \delta w_{11}^{[1]} + \cdots$. and $w_2^{[1]} = w_{10}^{[2]} + \delta w_{11}^{[2]} + \cdots$, with

$$w_{10}^{[1]} = \frac{1}{2^{15}\times 3^2 \times 5} r'(1 - r'^2) \times (19 - 21r'^2 + 9r'^4 - r'^6)\cos\theta, \tag{A16}$$

$$w_{11}^{[1]} = \frac{1}{2^{18}\times 3^3 \times 5^2}(1 - r'^2) \times [6(109 - 586r'^2 + 689r'^4 - 311r'^6 + 39r'^8) - 5r'^2(163 - 193r'^2 + 86r'^4 - 10r'^6)\cos 2\theta] \tag{A17}$$

and

$$w_{10}^{[2]} = 0, \tag{A18}$$

$$w_{11}^{[2]} = \frac{1}{2^{17}\times 3^2 \times 5^2}(1 - r'^2) \times [-(257 - 543r'^2 + 557r'^4 - 243r'^6 + 32r'^8) - 25r'^2(10 - 14r'^2 + 7r'^4 - r'^6)\cos 2\theta]. \tag{A19}$$

Some more equations for higher order derivations were shown, but the explicit solutions were not stated.

[1] S. Petersen, V. Peta, M. Rayner, J. Leal, R. Luengo-Fernandez, and A. Cray, *European Cardiovascular Disease Statistics 2005* (British Heart Foundation, London, 2005).

[2] S. Laurent, J. Cockcroft, L. Van Bortel, P. Boutouyrie, C. Giannattasio, D. Hayoz, B. Pannier, C. Vlachopoulos, I. Wilkinson, and H. Struijker-Boudier, "Expert consensus document onarterial stiffness: Methodological issues and clinical applications," Eur. Heart J. **27**, 2588 (2006).

[3] P. J. Brands, "Non-invasive methods for the assesment of wall shear rate and arterial impedance," Ph.D. thesis, University of Maastricht, 1996.

[4] P. J. Brands, A. P. G. Hoeks, L. A. F. Ledoux, and R. S. Reneman, "A radio frequency domain complex cross-correlation model to estimate blood flow velocity and tissue motion by means of ultrasound," Ultrasound Med. Biol. **23**, 911 (1997).

[5] J. W. Douchette, P. D. Corl, H. M. Payne, A. E. Flynn, M. Goto, M. Nassi, and J. Segal, "Validation of a Doppler guide wire for intravascular measurement of coronary artery flow velocity," Circulation **85**, 1899 (1992).

[6] G. F. Mitchell, H. Parise, J. A. Vita, M. G. Larson, E. Warner, J. F. Keaney, M. J. Keyes, D. Levy, R. S. Vasan, and E. J. Benjamin, "Local shear stress and brachial artery flow-mediated dilation: The framingham heart study," Hypertension **44**, 134 (2004).

[7] R. Krams, B. Bambi, F. Guidi, F. Helderman, A. F. W. van der Steen, and P. Tortoli, "Effect of vessel curvature on Doppler derived velocity profiles and fluid flow," Ultrasound Med. Biol. **31**, 663 (2005).

[8] S. Balbis, S. Roatta, and C. Guiot, "Curvature affects Doppler investigation of vessels: Implications for clinical practice," Ultrasound Med. Biol. **31**, 65 (2005).

[9] L. Liu, H. Zheng, L. Williams, F. Zhang, R. Wang, J. Hertzberg, and R. Shandas, "Development of a custom-designed echo particle image velocimetry system for multi-component hemodynamic measurements: system characterization and initial experimental results," Phys. Med. Biol. **53**, 1397 (2008).

[10] P. H. M. Bovendeerd, A. A. van Steenhoven, F. N. van de Vosse, and G. Vossers, "Steady entry flow in a curved pipe," J. Fluid Mech. **177**, 233 (1987).

[11] W. R. Dean, "The stream-line motion of fluid in a curved pipe," Philos. Mag. **5**, 673 (1928).

[12] H. C. Topakoglu, "Steady laminar flows of an incompressible viscous fluid in curved pipes," J. Math. Mech. **16**, 1321 (1967).

[13]J. H. Siggers and S. L. Waters, "Steady flows in pipes with finite curvature," Phys. Fluids **17**, 077102 (2005).
[14]D. J. McConalogue and R. S. Srivastava, "Motion of a fluid in a curved tube," Proc. R. Soc. London, Ser. A **307**, 37 (1968).
[15]W. M. Collins and S. C. R. Dennis, "The steady motion of a viscous fluid in a curved tube," Q. J. Mech. Appl. Math. **28**, 133 (1975).
[16]T. J. Pedley, *The Fluid Mechanics of Large Blood Vessels* (Cambridge University Press, Cambridge, 1980).
[17]A. J. Ward-Smith, *Internal Fluid Flow* (Clarendon, Oxford, 1980).
[18]S. A. Berger and L. Talbot, "Flow in curved pipes," Annu. Rev. Fluid Mech. **15**, 461 (1983).
[19]C. Cuvelier, A. Segal, and A. A. van Steenhoven, *Finite element methods and Navier-Stokes Equations* (Reidel, Dordrecht, 1986).
[20]G. Segal, *Sepran Introduction* (Ingenieursburea SEPRA, Den Haag, 1993).
[21]Y. Agrawal, L. Talbot, and K. Gong, "Laser anemometer study of flow development in curved circular pipes," J. Fluid Mech. **85**, 497 (1978).
[22]S. Murata, Y. Miyake, and T. Inaba, "Laminar flow in a curved pipe with varying curvature," J. Fluid Mech. **73**, 735 (1976).